AFRL-RX-WP-JA-2017-0354

IMPROVEMENTS IN THE PROCESSING OF POLYMER-DERIVED SIC MATRICES FOR CERAMIC MATRIX COMPOSITES (PREPRINT)

Derek S. King and Thomas S. Key

UES, Inc.

Zlatomir D. Apostolov, Carmen M. Carney, and Michael K. Cinibulk

AFRL/RX

9 January 2017
Interim Report

(STINFO COPY)

AIR FORCE RESEARCH LABORATORY
MATERIALS AND MANUFACTURING DIRECTORATE
WRIGHT-PATTERSON AIR FORCE BASE, OH 45433-7750
AIR FORCE MATERIEL COMMAND
UNITED STATES AIR FORCE

REPORT DOCUMENTATION PAGE

Form Approved
OMB No. 0704-0188

1. REPORT DATE *(DD-MM-YY)*	2. REPORT TYPE	3. DATES COVERED *(From - To)*
1 May 2017	Interim	23 September 2015 – 1 April 2017

4. TITLE AND SUBTITLE
IMPROVEMENTS IN THE PROCESSING OF POLYMER-DERIVED SIC MATRICES FOR CERAMIC MATRIX COMPOSITES (PREPRINT)

5a. CONTRACT NUMBER
FA8650-15-D-5230

5b. GRANT NUMBER

5c. PROGRAM ELEMENT NUMBER
62102F

6. AUTHOR(S)
1) Derek S. King and Thomas S. Key – UES
2) Michael K. Cinibulk– AFRL/RX

5d. PROJECT NUMBER
4347

5e. TASK NUMBER

5f. WORK UNIT NUMBER
X0Y2

7. PERFORMING ORGANIZATION NAME(S) AND ADDRESS(ES)
1) UES, Inc.
4401 Dayton Xenia Rd.
Beavercreek, OH 45432
2) AFRL/RX
Wright-Patterson AFB
Dayton, OH 45433

8. PERFORMING ORGANIZATION REPORT NUMBER

9. SPONSORING/MONITORING AGENCY NAME(S) AND ADDRESS(ES)
Air Force Research Laboratory
Materials and Manufacturing Directorate
Wright-Patterson Air Force Base, OH 45433-7750
Air Force Materiel Command
United States Air Force

10. SPONSORING/MONITORING AGENCY ACRONYM(S)
AFRL/RXCC

11. SPONSORING/MONITORING AGENCY REPORT NUMBER(S)
AFRL-RX-WP-JA-2017-0354

12. DISTRIBUTION/AVAILABILITY STATEMENT
Distribution Statement A. Approved for public release: distribution unlimited.

13. SUPPLEMENTARY NOTES
PA Case Number: 88ABW-2017-2113; Clearance Date: 1 May 2017. This document contains color. The U.S. Government is joint author of the work and has the right to use, modify, reproduce, release, perform, display, or disclose the work.

14. ABSTRACT *(Maximum 200 words)*
The rheological properties of commercially available polycarbosilane, SMP-10, were analyzed as a function of temperature, to guide development of thermal treatment processes for the improved yield and functionality of polymer ceramic precursors. The curing onset temperature for SMP-10 was determined to be as low as 100°C for a heating rate of 1°C/min enabling a heat treatment process at 90°C that volatilizes low molecular weight oligomers from the liquid precursor. By driving off the low molecular weight oligomers before fabrication of a composite, the mass yield of SMP-10, from a room temperature liquid state was increased from 77% to 83%. The utilization of B-staging processes, or a semi-cure of SMP-10, was also demonstrated. B-staging processes were then applied to polymer infiltration and pyrolysis processing, where itwas determined that B-staging processes did not adversely affect ceramic matrix composite fabrication. By employing B-staging, the ability to engineer two dimensional composite matrices with ply-by-ply control of the microstructural composition was demonstrated.

15. SUBJECT TERMS
polycarbosilane, SMP-10; polymer ceramic; curing onset temperature; molecular weight oligomer; B-staging process

16. SECURITY CLASSIFICATION OF:			17. LIMITATION OF ABSTRACT:	18. NUMBER OF PAGES	19a. NAME OF RESPONSIBLE PERSON (Monitor)
a. REPORT	b. ABSTRACT	c. THIS PAGE			Ming Chen
Unclassified	Unclassified	Unclassified	SAR	29	19b. TELEPHONE NUMBER *(Include Area Code)* (937) 255-9821

Improvements in the Processing of Polymer-Derived SiC Matrices for Ceramic Matrix Composites

Derek S. King[1,2], Zlatomir D. Apostolov[1], Thomas S. Key[1,2], Carmen M. Carney[1], Michael K. Cinibulk[1]

[1]Air Force Research Laboratory, Materials and Manufacturing Directorate,
Wright-Patterson Air Force Base, OH, 45433, USA

[2]UES, Inc.
Dayton, OH, 45432, USA

ABSTRACT

The rheological properties of commercially available polycarbosilane, SMP-10, were analyzed as a function of temperature, to guide development of thermal treatment processes for the improved yield and functionality of polymer ceramic precursors. The curing onset temperature for SMP-10 was determined to be as low as 100°C for a heating rate of 1°C/min enabling a heat treatment process at 90°C that volatilizes low molecular weight oligomers from the liquid precursor. By driving off the low molecular weight oligomers before fabrication of a composite, the mass yield of SMP-10, from a room temperature liquid state was increased from 77% to 83%. The utilization of B-staging processes, or a semi-cure of SMP-10, was also demonstrated. B-staging processes were then applied to polymer infiltration and pyrolysis processing, where it was determined that B-staging processes did not adversely affect ceramic matrix composite fabrication. By employing B-staging, the ability to engineer two dimensional composite matrices with ply-by-ply control of the microstructural composition was demonstrated.

INTRODUCTION

In order to enable the use of fiber-reinforced ceramic matrix composites (CMCs) in extreme environments, matrix selection becomes an important factor when considering CMC implementation.[1] In a hypersonic flight environment, temperatures may exceed 2000°C; therefore, UHTCs, like HfB_2, are desired for their high melting temperature, high thermal conductivity, and oxidation resistance.[2-4] The common CMC processing routes that can be used

to introduce such UHTC refractory materials into the matrix include: melt-infiltration (MI), chemical vapor infiltration (CVI), and polymer infiltration and pyrolysis (PIP). MI matrices typically suffer from choking reactions, which can prohibit the full reaction of the metal infiltrant with other matrix components, leaving residual low melting temperature metal in the matrix.[5] The main advantage of CVI is the ability to obtain fully crystalline matrices, but CVI processes can be slow and costly, and often lead to a highly porous matrix with large angular porosity that can be detrimental to cyclic fatigue behavior.[6, 7] Similarly, the numerous re-infiltration steps required for PIP processing can result in limited matrix density, while also being time consuming. More notably, the processing temperatures required to achieve full matrix crystallinity from pre-ceramic polymers (PCPs) can lead to degradation of SiC fibers.[8-10]

In order to minimize time and porosity, a focus is placed on a high ceramic yield (>50% by weight) during PIP processing, where a higher mass yield is desired for the production of more ceramic material. Ideally, pre-ceramic polymers should have sufficiently high molecular weight (MW) and a narrow MW distribution, in order to prevent small oligomer volatilization during heat treatment.[11, 12] In practice, a wide distribution of molecular weights are typically observed in commercial pre-ceramic polymers, where volatile low molecular weight species are present in significant amounts. Sreeja et al. suggested that low MW oligomers can be driven out of SMP-10 at curing temperatures as low as 200°C.[13] Li et al. also discussed that at temperatures below 230°C, the release of H_2 gas and small oligomers are the primary factors contributing to mass loss of a similar liquid polycarbosilane (LPCS).[14] Similarly, Zhao et al. attributed mass loss of their LPCS between 50-250°C to loss of low MW molecules.[15] The wide MW distributions of these LPCSs (including SMP-10) brings into question whether low MW oligomers, that would be lost during curing, can be driven off thermally, while the polymer is still in a liquid state; the potential payoff is a pre-ceramic polymer that can be used for PIP processing with a higher ceramic yield and a ceramic chemistry that has not been altered by the use of polymer catalysts.

Other low temperature behaviors can also be investigated for thermoset PCPs, such as partial curing, or B-staging. When the polymer exhibits no cross-linking, it is in an A-stage, and a fully cross-linked polymer is in a C-stage.[16] The period between the A and C-stage, where the degree of cross-linking and polymer rigidity varies, is referred to as the B-stage.[16, 17] In PMC fabrication, B-staging is an established processing method that can be used to control polymer behavior after infiltration into a fabric.[18-23] Similar processing of thermoset pre-ceramic polymers for the fabrication of CMCs has not been reported.

The goals of the study presented herein were to develop improvements to polymer yield and handleability during PIP processing of CMCs, through the investigation of the low temperature behavior of the commercially available polycarbosilane, SMP-10. Viscosity, thermogravimetric analysis (TGA), and gel permeation chromatography (GPC) analysis' were coupled with heat treatment experiments in order to better understand the curing and pyrolysis behavior of SMP-10. It was determined that the ceramic yield of the polymer can be significantly enhanced by a tailored pre-treatment. The development of B-staging processes presents the opportunity to control compositional gradients throughout the CMC through placement and retention of a particulate filler; therefore, CMCs with graded matrices were fabricated using the conventional wet layup method and using a B-staged fabric, where SiC and HfB_2 particulates were utilized for the fabrication of conventional and UHTC matrices within the same composite. A comparison of the resulting microstructures was used to elicit processing/microstructure relationships. Utilizing SMP-10 in this modified state resulted in a more convenient layup routine, while providing desired control over the design of matrix compositions.

EXPERIMENTAL PROCEDURE

Commercially available polycarbosilane (StarPCS™ SMP-10; Starfire Systems, Inc., Schenectady, NY) was analyzed using dynamic rheology measurements (ARES-G2; TA Instruments, New Castle, DE), while heating at a rate of 1°C/min, to a temperature of 250°C. Isothermal rheology measurements were taken after heating at a rate of 1°C/min, to a temperature

of 100°C and collecting data for an isothermal hold time of 20 h. Rheological data was acquired at a constant angular frequency of 6.28 rad/s. Thermogravimetric analysis (SDT Q600; TA Instruments, New Castle, DE) was performed on as-received SMP-10 and after various stages of vacuum heat treatment, where liquid SMP-10 was placed in an alumina cup and heated at a rate of 1°C/min under flowing argon (100 mL/min) to the final analysis temperature. Molecular weight distribution measurements were carried out on SMP-10, dispersed in tetrahydrofuran (THF) as the carrier liquid, via gel permeation chromatography (Agilent 1260; Agilent Technologies, Santa Clara, CA), using a refractive index detector (Wyatt Optilab T-rex; Wayatt Technology, Santa Barbara, CA). The rheology, TGA, and molecular weight distribution results were used to guide selection of SMP-10 processing parameters.

Heat treatment of SMP-10 was performed in a vacuum oven (OV-11; Jeio Tech, Billerica, MA) by heating at a rate of 1°C/min and holding at the treatment temperature for varying times. The vacuum atmosphere was intended to assist with removal of low MW oligomers in larger lots, 100s of grams compared to the 10s of milligrams that could be studied with TGA. It should be noted that because of the difference in experimental environment, such as temperature distribution, atmosphere, or sample geometry, the heat treatment of SMP-10 in a vacuum oven was not expected to perfectly match the flowing argon atmosphere heat treatment experiments performed in the TGA. Specimens heat treated at 86°C were analyzed at ~2.5 h increments using GPC, while specimens' heat treated at 90°C were analyzed using TGA.

Powders of SiC (<1 µm, 99.9%; Materion Advanced Chemicals, Milwaukee, WI) and a 1:1 (by volume) mixture of SiC and HfB_2 (-325 mesh, 99.5%; Materion) were ball-milled, with SiC milling media, for 2 h in isopropyl alcohol to break up agglomerates in the as-received powder. After milling, the powder slurries were dried using rotary evaporation and sieved to -60 mesh. Powders were then mixed with heat treated SMP-10 (HT SMP-10) in a planetary mixer (ARV-310, THINKY USA, Laguna Hills, CA). The slurries were infiltrated into a SiC fiber fabric (Hi-Nicalon™ Type S; COI Ceramics, Inc., San Diego, CA) (8H satin weave, woven by T.E.A.M., Inc.,

Woonsocket, RI), using a laboratory laminator (Laboratory Laminator; ChemInstruments, West Chester, OH) set to accommodate the thickness of the fabric and supporting sheets of Teflon™. Prior to polymer infiltration, the woven fabric was coated with BN and then SiC, applied by CVI (Rolls-Royce High Temperature Composites, Inc., Huntington Beach, CA). Infiltrated fabrics were either cut into squares, nominally 5 cm by 5 cm (2 in. by 2 in.), for conventional layup or B-staged and then cut to size for layup. In subsequent discussion, non B-staged fabrics will be referred to as "wet". Initial B-staging experiments were carried out by infiltrating Nextel™ 610 fabric with vacuum heat treated SMP-10 and heated at a rate of 1°C/min, to a temperature of 95°C, in a vacuum oven for 2, 5, 10, and 20 h, in-order-to determine the parameters necessary for obtaining B-staged fabric that could be used for a CMC layup. B-staging of powder loaded and infiltrated fabric was completed by heating under vacuum at a heating rate of 1°C/min to 95°C, and holding for 70 min. B-staged fabrics were removed from the vacuum oven during cooling at ~80°C, and cut to the same nominal size as the wet fabric, for layup. Wet and B-staged CMCs were fabricated with a $[0/90/0]_s$ architecture. For both layups, the top two SiC fabric plies were initially infiltrated with HT SMP-10/HfB_2-SiC particulate slurry, while the bottom four plies were initially infiltrated with HT SMP-10/SiC particulate slurry.

Consolidation of the 2D layups was completed by an autoclave step. Layups were placed in a vacuum bag and heated at a rate of 1°C/min in an autoclave (EC-2X4-200P800F2S2P4T; ASC Process Systems, Chatsworth, CA). At a temperature of 100°C, an external pressure of ~690 kPa (100 psi) was applied to the outside of the bag, while the inside of the bag remained under vacuum. Heating continued at a rate of 0.75°C/min to a final temperature of 250°C where the layups were isothermally held for 1h. As a result of autoclaving, the layup became consolidated, such that it could no longer be disassembled layer by layer; therefore, further discussion will refer to an autoclaved layup as a "laminate". The autoclaved laminate was cooled at a rate of ~5.6°C/min to RT, where pressure was released at a temperature of 60°C.

Densification of the wet and B-staged laminates followed conventional PIP processing. After autoclave consolidation, laminates were pyrolyzed by heating at a rate of 5°C/min to a temperature of 1300°C, under a flowing argon atmosphere, in a graphite element furnace (F-14X14X14-GG-2500-VM-G; Materials Research Furnaces, Inc., Allenstown, NH). Laminates were held at 1300°C for 1 h. The pyrolyzed laminates were vacuum re-infiltrated with HT SMP-10. Re-infiltrated specimens were heated in a vacuum oven (DZF-6050-HT/500; MTI Corporation, Richmond, CA) at a rate of 1°C/min to a temperature of 250°C and held for 3 h to cure the HT SMP-10, before subsequent pyrolysis. A total of six re-infiltrations were performed.

Microscopy of CMC laminate cross-sections was accomplished using light microscopy (Axio Observer.Z1m; Carl Zeiss Microscopy, LLC, Thornwood, NY) and scanning electron microscopy (Quanta FEG 650; FEI Company, Hillsboro, OR). Image analysis was performed using ImageJ software (National Institute of Health, Bethesda, MD).

RESULTS AND DISCUSSION

SMP-10 Heat Treatment

Rheological measurements aimed at establishing the cure onset temperature (T_{cure}) of SMP-10 were used to determine a temperature for heat treatment where SMP-10 would remain inviscid while low MW oligomers would be removed. T_{cure} was determined to be the temperature at which a drastic increase in viscosity occurred.[24] Dynamic heating rheology experiments revealed a difference in T_{cure} based on heating rate (Figure 1). At a heating rate of 1°C/min, a T_{cure} of 103°C was observed, while at a rate of 2.75°C/min, a T_{cure} of 114°C was observed. For both heating rates, it was also observed that the viscosity of SMP-10 rapidly increased to values $>10^4$ Pa·s once T_{cure} was surpassed. As T_{cure} was observed to be as low as 103°C, an isothermal rheology experiment was then conducted in order to mimic an isothermal heat treatment of SMP--10 at 100°C. The isothermal viscosity measurements, presented in Figure 2, revealed an increase in SMP-10 viscosity from a range of 0.1 to 0.6 Pa·s to $>10^3$ Pa·s in <10 min. Both sets of rheology experiments support previous reports of low temperature curing (<200°C) for LPCS;

however, it was determined that curing of SMP-10 can be initiated at temperatures as low as 100°C.

Based on rheology results, TGA was utilized to measure the change in mass of SMP-10 during heat treatments. A temperature of 90°C was chosen with the intent of maximizing mass loss and avoiding curing. Presented in Figure 3, TGA of SMP-10 at 90°C for 48 h revealed rapid initial mass loss (10 wt% in ~4.5 h) that slowed over time (4 wt% over the final ~43.5 h) but continued throughout the entire 48 h hold. A total mass loss of ~14 wt% was observed. The observed mass loss presented the potential to improve the yield of as-received SMP-10; however, it was also observed that SMP-10 had crossed its gel-point and was no longer inviscid after 48 h at 90°C. Without an inviscid polymer, that can also be infiltrated, a pre-treatment processes step would not be beneficial. Therefore, additional TGA runs were conducted to elucidate that SMP-10 remained an inviscid liquid at 90°C for isothermal holds up to 10 h in length, where a mass loss of ~12 wt% was observed.

To confirm that the mass loss from SMP-10 was mostly due to the volatilization of smaller polymer segments, i.e. low MW oligomers, rather than dominated by scission of larger molecules, gel permeation chromatography (GPC) was performed on various SMP-10 specimens to measure the effect of an 86°C vacuum heat treatment on the average MW of SMP-10. It should be noted that the previous heat treatment temperature was 90°C, as opposed to 86°C for GPC analysis; therefore, longer heat treatment times were accessible, while limiting the chances of gelling the SMP-10. Via GPC, the cumulative mass distribution of SMP-10 was measured as a function of molar mass, then differentiated and plotted as the linear differential molar mass as a function of molar mass (Figure 4). In the Figure 4 plot, the peak linear differential molar mass shifted to larger MW values with increasing treatment time, where the peak MW was 290 g/mol for as-received SMP-10 and increased to 380 g/mol after a 15 h heat treatment. Similarly, as treatment time increased, the concentration of a specific molar mass was observed to decrease. In Figure 4, this was depicted with a straight line at a molar mass of 200 g/mol, where the

decreasing linear differential molar mass can be correlated to a decrease in the concentration of polymer chains at 200 g/mol in the cumulative mass distribution. It was also observed that the GPC curves converged at a molar mass of ~1000 g/mol. With an increase in the peak MW, a drop in concentration at low MW, and a convergence of GPC curves at higher MW, it was concluded that heat treatments were indeed allowing the volatilization of low MW oligomers from SMP-10 before the onset of curing/cross-linking. This conclusion is consistent with previous work on LPCS; however, the loss of low MW oligomers for this study occurred at temperatures (86°C) much lower than previously reported (230°C).[14, 15]

TGA was also used to compare the ceramic yield of heat treated SMP-10 with that of as-received SMP-10, at a pyrolysis temperature of 1200°C. The TGA data were plotted and are presented in Figure 5. The plot revealed that as-received SMP-10 (As Received 1) started losing mass from the start of the TGA run, while the HT SMP-10 (HT1) did not begin to lose mass until ~50°C. Overall, as-received SMP-10 exhibited a mass loss of ~28 wt%, while HT SMP-10 exhibited a mass loss of ~19 wt%. A vacuum heat treatment step was adopted, resulting in the increase of SMP-10 ceramic yield, from 72 wt% (as-received) to 81 wt% (heat-treated); a percent increase in ceramic yield of ~13% at 1200°C.

A review of previous TGA studies on SMP-10 revealed that the yield of the as-received SMP-10 analyzed in this study was at the low end of the yield range reported for SMP-10 pyrolyzed to ≥900°C (~72-77%).[13, 25-28] Therefore, a second sample, from a different lot, of SMP-10 was analyzed with TGA in order to gain insight into the reported variability of the ceramic yield of SMP-10. The TGA behavior of the second lot did not duplicate the behavior of the first lot. Comparison of the TGA behavior for both lots is presented in Figure 5. It was observed that for the second lot (As Received Lot 2), the ceramic yield at 1200°C was ~77 wt%, compared to a yield of ~72 wt% for “As Received Lot 1”, a percent difference of ~7%. TGA of the low temperature heat treatment (90°C, 10 h) of the second lot revealed a mass loss of ~10 wt%, compared to the ~12 wt% of Lot 1. This was a difference of 18% between the two lots. Consistent with the

difference between the As Received Lots, the ceramic yield of the second lot after vacuum heat treatment (HT2 in Figure 5) also differed from that of Lot 1. With a ceramic yield of ~83 wt%, HT2 differed from HT1's yield of ~81 wt%. To the authors' knowledge, these yields are the highest reported ceramic yield for liquid SMP-10 (i.e. non-cured SMP-10 before pyrolysis) without the addition of catalysts or other chemical modification of the pre-ceramic polymer.[28] Although lot variability was observed for SMP-10, vacuum heat treatment was capable of increasing the ceramic yield of SMP-10 without the use of chemical modification.

The observed lot variability of SMP-10 was thought to be due to differences in the low MW distributions of different SMP-10 lots, where it has been concluded that low temperature mass loss was governed by the loss of low MW oligomers. In turn, these differences can be reflected in the non-uniform response of the polymer to identical treatments, making their behavior during processing unpredictable.

B-staging SMP-10

Previous viscosity measurements (Figure 1 and Figure 2) and heat treatment experiments were utilized as a guide to develop B-staging parameters. First, dynamic heating was observed to lead to a sudden increase in viscosity, resulting in a polymer state beyond that suitable for CMC processing. Second, it was determined that a 100°C isothermal treatment could be too aggressive, where SMP-10 may quickly (<15 min) reach a state not suitable for further processing (Figure 2). Third, heat treatment experiments at 86°C revealed that a gel-like "skin" developed on heat treatment specimens with a high surface area to volume ratio, e.g. an infiltrated fiber weave. The time needed to form such a skin was typically >15 h; therefore, it was determined that a temperature window was available for the B-staging of SMP-10, such that B-staged fiber weaves are solid, flexible, and amenable to autoclave processing.

After B-staging Nextel 610™ fabric for various times, the fabric was placed in a graphite mold to determine flexibility/conformability of the B-staged fabric, when compared to as-received (dry) fabric (Figure 6). Figure 6a depicts a dry fabric, i.e., a fabric that has not been infiltrated with

liquid SMP-10.. The fabric presented in Figure 6b was B-staged for 2 h. Like the dry fabric, the 2 h B-staged fabric deformed under the weight of the graphite and conformed to all of the mold contours. At this stage the infiltrated polymer had gelled, but remained soft within the fabric and had some tack. Additionally, no cracks or bare fiber spots were formed upon deformation or after removal from the mold; a small amount of polymer residue was left on the graphite mold, which could be beneficial for ply consolidation during autoclave processing. As the B-staging time was increased to 5 h, the conformability of the fabric was lost. In Figure 6c, the graphite mold deformed the 5 h B-staged fabric, but without the same mold conformation as the 2 h B-staging treatment. The gap between the fabric and mold was measured to be ~5 mm. Similarly, the 10 h (Figure 6d) and 20 h (Figure 6e) B-staged fabrics retained some flexibility, but could not conform to the mold. The gap between the fabric and the graphite mold increased from ~13 mm (10 h B-stage), to ~15 mm (20 h B-stage). While the gap measurements for the 5, 10, and 20 h may not be quantifiable for other purposes, the increasing gap size demonstrated that the B-staging process can result in fabrics with varying degrees of SMP-10 cure.

Finally, as previously discussed, the fabric must be amenable to autoclaving for the B-staging processes to be useful. As only the 2 h B-staging process resulted in compliant and conformable infiltrated fabric, plies of 2 h B-staged fabric were pressed between two heated platens, at ~200°C, to simulate autoclave lamination. This resulted in a single laminate, where bonding of the plies was attributed to the low degree of cure after 2 h B-staging, where SMP-10 within the plies was perceived as a soft and pliable gel. For comparison, 5 h B-staged fabric plies were heated and pressed together; however ply bonding was not achieved and the laminate pulled apart during handling. By controlling the degree of cure through thermal treatments, B-staging of SMP-10 infiltrated fabric was demonstrated.

CMC Processing and Microstructure

Powder loaded SMP-10 was observed to reach the desired B-stage for layup quicker than the non-loaded powder, where a 90 min B-staging step resulted in a “dry to the touch” fabric that

no longer had tack. This was likely due to the surface area dependence on curing that was described in the B-staging subsection. That is, while the specific surface area of the infiltrated weave remained constant, the volume fraction of the polymer present in the weave was decreased due to the powder loading, effectively increasing the specific surface area of the polymer. Therefore, B-staging times for powder/SMP-10 infiltrated plies were decreased to 70 minutes and the resulting B-staged fabric was tacky, as previously discussed. After B-staging, lamination of the wet and B-staged plies was performed by autoclaving, where it was observed that polymer slurry was squeezed from the wet laminates during autoclaving; the same behavior was not observed from the B-staged laminates. The fluid motion of the slurry within the wet laminates suggested that mixing likely occurred between the powder loaded plies, where neighboring plies containing HfB_2 or SiC particulates would be affected through a change in the designed matrix composition. CMC densification was then carried out via conventional PIP processing methods. The percent mass change between each PIP cycle was recorded and compared for both CMCs and plotted in the Figure 7 graph. The data revealed similar mass changes between re-infiltration steps, for both CMCs, with a total mass gain of ~42% for both layups. Similarly, the final densities, calculated using the Archimedes' method, were 2.93 g/cm^3 for the wet and 2.94 g/cm^3 for the B-staged laminates. Laminate thicknesses were measured to be ~2.4mm for wet and ~2.3 mm for B-staged. Fiber volume fractions were also calculated to be ~28% and ~29% for the wet and B-staged laminates, respectively. The similar bulk density, thickness, and fiber volume fraction of both laminates suggested that the nominal compositions of both laminates remained the same. It was concluded that processing of wet and B-staged CMC laminates result in nominally identical macro structures.

Polished cross-sections of the wet and B-staged laminates were analyzed using light microscopy, and micrographs are presented in

Figure 8. Due to the limited contrast between the polymer-derived SiC matrix and SiC particulate, the area fractions of HfB_2 particulate were analyzed in order to determine the effect

of powder loading as well as determine if mixing between HfB_2 and SiC loaded polymer occured. Indeed, microstructural analysis revealed that, HfB_2 loaded slurries migrated between plies of the wet laminate. However, the measured area fraction of HfB_2 content was higher than the 15 vol% HfB_2 content used for SMP-10 powder loading. It was determined that the particulate did not infiltrate the fiber tows during polymer loading, resulting in higher particulate loading within interlaminar regions of the laminate. Occurring in both wet and B-staged laminates, such areas were identified in

Figure 8, where arrows distinguish SiC fiber tows surrounded by the HfB_2 rich interlaminar regions. It should also be noted, that as the SiC fabric for both laminates was loaded on a ply-by-ply basis, the resulting B-staged laminate represents the desired final microstructure with respect to initial design (2 plies of HfB_2 loading, 4 plies of SiC loading). Plotted as a function of depth from the surface, the HfB_2 content of the wet and B-staged laminates was compared through Figure 9. For the wet laminate, HfB_2 content was measured to be ~25% at a depth of 50 µm from the surface, ~30% between 150 to 600 µm, and ~25% beyond a depth of ~700 µm from the surface. Further analysis of the wet laminate revealed that HfB_2 content continued to decrease, with increasing distance from the laminate surface, where HfB_2 content was ~19% at a depth of 1mm and ~10% at 1.5 mm below the laminate surface. Ultimately, HfB_2 particulate was observed as deep as ~1.7 mm from the surface of the ~2.4 mm thick wet laminate. In contrast, the measured HfB_2 content for the B-staged laminate was ~30% over the thickness of the two HfB_2 loaded plies, an overall depth of ~800 µm from the surface for the ~2.3 mm thick laminate; HfB_2 was not observed below a depth of 800 µm. It was also observed that dispersion of HfB_2 within the top ~700 µm of the wet laminate was also observed to be relatively uniform; however, as HfB_2 content decreased settling of the particulate in interlaminar regions was observed. Figure 10, depicts such a region within the wet laminate (interlaminar span of ~0.7 to ~0.75 mm from the surface), where HfB_2 particulate had settled, resting on the transverse tow at the bottom of the figure. This resulted in a higher volume fraction of HfB_2 at the interface of the

transverse tow (~36 vol%) compared to the matrix between it and the orthogonal tow at the top of the figure (~3 vol%). The settling of HfB_2 in the wet laminate may also explain the increasing error in measured HfB_2 content for the wet laminate, where migration of HfB_2 particulate in the wet laminate led to increased variation in the measured area fraction of HfB_2 for different images taken at the same nominal depth from the laminate surface. It should be noted that the time in between layup and autoclave was ~15 h, and therefore, it is unknown if an immediate autoclave step would have prevented the settling of HfB_2; nevertheless, it is important to note that HfB_2 was not observed to settle in the B-staged laminate. Therefore, the time difference between layup and autoclave highlights that time sensitivity may be critical when utilizing a wet layup process, but the gelled nature of SMP-10 used in the B-staged processing would allow an essentially time independent process where engineered ply-by-ply compositional control can be accomplished.

CONCLUSIONS

Rheological measurements were used to identify the onset of curing, at a heating rate of 1 °C/min, where increases in the viscosity of SMP-10 indicated that curing of SMP-10 could be accomplished as low as 100°C. Based on rheological measurements, TGA experiments revealed that SMP-10 could be heat-treated for a time of 10 h at 90°C, while preventing curing. In a vacuum oven, heat treatment process resulted in a mass yield of 83% and 81% for heat-treated SMP-10, compared with 77% and 72% for two different lots of as-received SMP-10. GPC revealed that low molecular weight oligomers can be driven off of SMP-10 at temperatures below the onset of curing, and that variations between the MW distribution of SMP-10 will affect the heat treatment behavior. Understanding of the low temperature behavior of SMP-10 guided the development of B-staging process, where the use of a B-staged SMP-10 allowed processing styles similar to polymer matrix composites, rather than conventional wet CMC layup processing. It was concluded that B-staging did not adversely affect the PIP processing of CMCs, while providing a time independent layup process, and providing the ability to engineer CMC matrices on a ply-by-ply level.

ACKNOWLEDGEMENTS

The authors thank Mr. Randy Corns for his assistance with autoclave and furnace operations, as well as Ms. Bridget Larson and Mr. Patrick Kazmeirski for their assistance with ceramographic preparations and imaging. This work was funded under United States Air Force Contracts FA8650-10-D-5226 and FA8650-15-D-5230.

REFERENCES

1. J. Marschall, D. Pejakovic, W. G. Fahrenholtz, G. E. Hilmas, F. Panerai, and O. Chazot, "Temperature Jump Phenomenon During Plasmatron Testing of ZrB_2-SiC Ultrahigh-Temperature Ceramics," *J. Thermophys. Heat Transfer,* **26**[4] 559-72 (2012).
2. W. G. Fahrenholtz, G. E. Hilmas, I. G. Talmy, and J. A. Zaykoski, "Refractory Diborides of Zirconium and Hafnium," *J. Am. Ceram. Soc.,* **90**[5] 1347-64 (2007).
3. T. A. Parthasarathy, R. A. Rapp, M. Opeka, and R. J. Kerans, "A model for the oxidation of ZrB_2, HfB_2 and TiB_2," *Acta Mater.,* **55**[17] 5999-6010 (2007).
4. C. Carney, C. Leslie, and E. Jones, "Oxidation of SiC_f/SiC-HfB_2 Composites under Laser Heating," *Int. J. Appl. Ceram. Technol.,* **13**[2] 295-301 (2016).
5. A. Favre, H. Fuzellier, and J. Suptil, "An original way to investigate the siliconizing of carbon materials," *Ceram. Int.,* **29**[3] 235-43 (2003).
6. J. E. Webb, R. N. Singh, and R. A. Lowden, "Thermal Shock Damage in a Two-Dimensional Woven-Fiber-Reinforced-CVI SiC-Matrix Composite," *J. Am. Ceram. Soc.,* **79**[11] 2857-64 (1996).
7. W. Yang, T. Noda, H. Araki, J. Yu, and A. Kohyama, "Mechanical properties of several advanced Tyranno-SA fiber-reinforced CVI-SiC matrix composites," *Materials Science and Engineering: A,* **345**[1–2] 28-35 (2003).
8. Y. Hu, F. Luo, S. Duan, W. Zhou, and D. Zhu, "Mechanical and dielectric properties of SiC_f/SiC composites fabricated by PIP combined with CIP process," *Ceram. Int.,* **42**[6] 6800-06 (2016).
9. S. Kaur, G. Cherkashinin, C. Fasel, H.-J. Kleebe, E. Ionescu, and R. Riedel, "Single-source-precursor synthesis of novel V_8C_7/SiC(O)-based ceramic nanocomposites," *J. Eur. Ceram. Soc.,* **36**[15] 3553-63 (2016).
10. T. A. Parthasarathy, C. P. Przybyla, R. S. Hay, and M. K. Cinibulk, "Modeling Environmental Degradation of SiC-Based Fibers," *J. Am. Ceram. Soc.,* **99**[5] 1725-34 (2016).
11. M. Birot, J.-P. Pillot, and J. Dunogues, "Comprehensive Chemistry of Polycarbosilanes, Polysilazanes, and Polycarbosilazanes as Precursors of Ceramics," *Chem. Rev. (Washington, DC, U. S.),* **95**[5] 1443-77 (1995).
12. Z. Yu, H. Min, L. Yang, Y. Feng, P. Zhang, and R. Riedel, "Influence of the architecture of dendritic-like polycarbosilanes on the ceramic yield," *J. Eur. Ceram. Soc.,* **35**[4] 1161-71 (2015).
13. R. Sreeja, B. Swaminathan, A. Painuly, T. V. Sebastian, and S. Packirisamy, "Allylhydridopolycarbosilane (AHPCS) as matrix resin for C/SiC ceramic matrix composites," *Materials Science and Engineering: B,* **168**[1–3] 204-07 (2010).
14. H. Li, L. Zhang, L. Cheng, Y. Wang, Z. Yu, M. Huang, H. Tu, and H. Xia, "Effect of the polycarbosilane structure on its final ceramic yield," *J. Eur. Ceram. Soc.,* **28**[4] 887-91 (2008).
15. S. Zhao, Z. Yang, and X. Zhou, "Microstructure and Mechanical Properties of Compact SiC/SiC Composite Fabricated with an Infiltrative Liquid Precursor," *J. Am. Ceram. Soc.,* **98**[4] 1332-37 (2015).
16. "Handbook of Thermoset Plastics," pp. 800. William Andrew: San Diego, CA, (2013).
17. A. E. Hoyt and B. C. Benicewicz, "Rigid rod molecules as liquid crystal thermosets. II. Rigid rod esters," *J. Polym. Sci. A Polym. Chem.,* **28**[12] 3417-27 (1990).
18. M. Krumova, C. Klingshirn, F. Haupert, and K. Friedrich, "Microhardness studies on functionally graded polymer composites," *Composites Science and Technology,* **61**[4] 557-63 (2001).
19. S. Kumar, K. V. V. S. Murthy Reddy, A. Kumar, and G. Rohini Devi, "Development and characterization of polymer–ceramic continuous fiber reinforced functionally graded composites for aerospace application," *Aerospace Science and Technology,* **26**[1] 185-91 (2013).

20. G. L. Warren, L. Sun, V. G. Hadjiev, D. Davis, D. Lagoudas, and H.-J. Sue, "B-staged epoxy/single-walled carbon nanotube nanocomposite thin films for composite reinforcement," *J. Appl. Polym. Sci.,* **112**[1] 290-98 (2009).
21. V. J. Lopata, C. B. Saunders, A. Singh, C. J. Janke, G. E. Wrenn, and S. J. Havens, "Electron-beam-curable epoxy resins for the manufacture of high-performance composites," *Radiat. Phys. Chem.,* **56**[4] 405-15 (1999).
22. J. B. Henderson and T. E. Wiecek, "A numerical study of the thermally-induced response of decomposing, expanding polymer composites," *Wärme - und Stoffübertragung,* **22**[5] 275-84 (1988).
23. E. B. Stark, A. M. Ibrahim, T. E. Munns, and J. C. Seferis, "Moisture effects during cure of high-performance epoxy matrices," *J. Appl. Polym. Sci.,* **30**[4] 1717-31 (1985).
24. C.-Y. M. Tung and P. J. Dynes, "Relationship between viscoelastic properties and gelation in thermosetting systems," *J. Appl. Polym. Sci.,* **27**[2] 569-74 (1982).
25. J. Zheng, M. J. Kramer, and M. Akinc, "In situ Growth of SiC Whisker in Pyrolyzed Monolithic Mixture of AHPCS and SiC," *J. Am. Ceram. Soc.,* **83**[12] 2961-66 (2000).
26. Y.-S. Jang, M. Jank, V. Maier, K. Durst, N. Travitzky, and C. Zollfrank, "SiC ceramic micropatterns from polycarbosilanes," *J. Eur. Ceram. Soc.,* **30**[13] 2773-79 (2010).
27. S. Kaur, R. Riedel, and E. Ionescu, "Pressureless fabrication of dense monolithic SiC ceramics from a polycarbosilane," *J. Eur. Ceram. Soc.,* **34**[15] 3571-78 (2014).
28. S. Kaur, G. Mera, R. Riedel, and E. Ionescu, "Effect of boron incorporation on the phase composition and high-temperature behavior of polymer-derived silicon carbide," *J. Eur. Ceram. Soc.,* **36**[4] 967-77 (2016).

LIST OF FIGURES

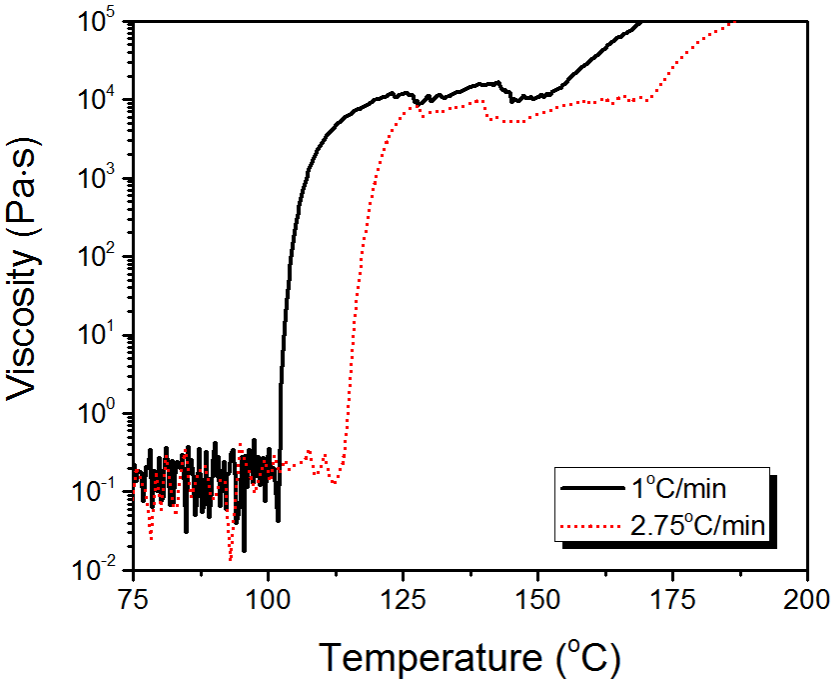

Figure 1. Measurement of SMP-10's shear viscosity, under dynamic heating conditions, through the onset of curing for two heating rates.

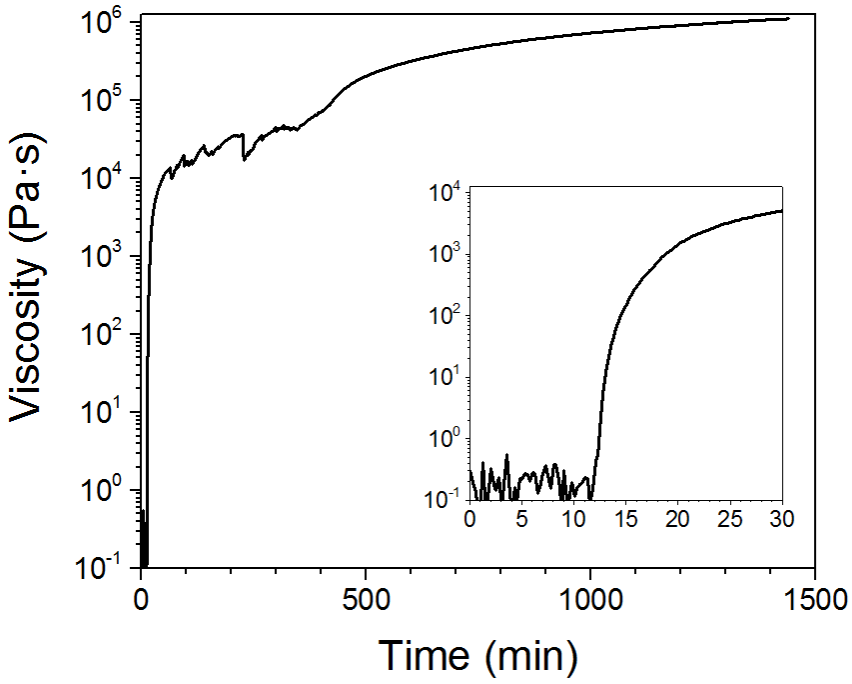

Figure 2. Shear viscosity of SMP-10 as a function of time at 100°C, measured using a constant angular frequency of 6.28 rad/s.

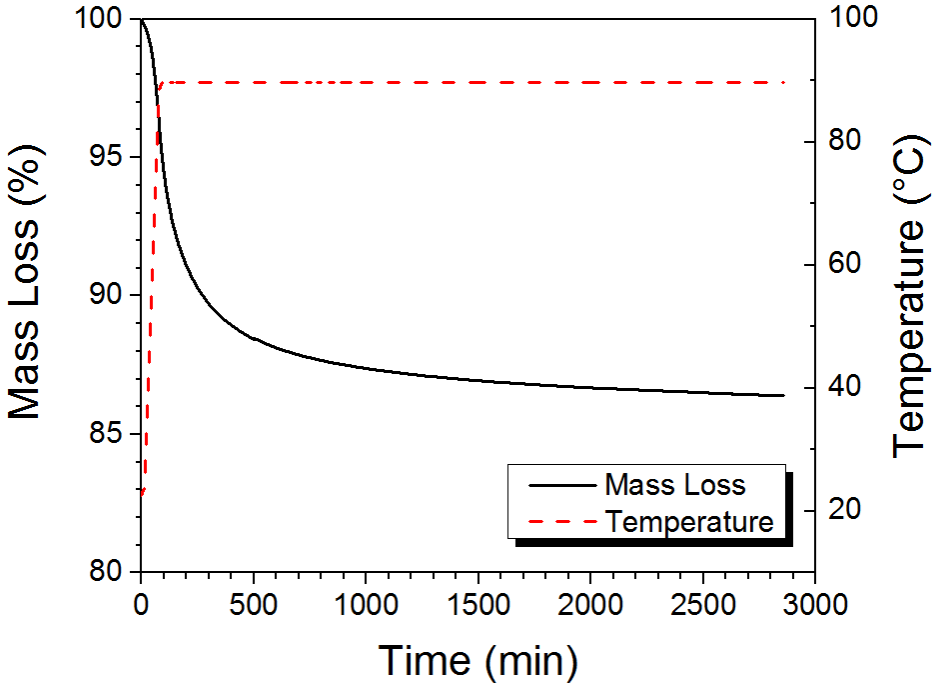

Figure 3. TGA of SMP-10 mass loss, during a 48 h hold at 90°C, revealing a total mass loss of ~14%.

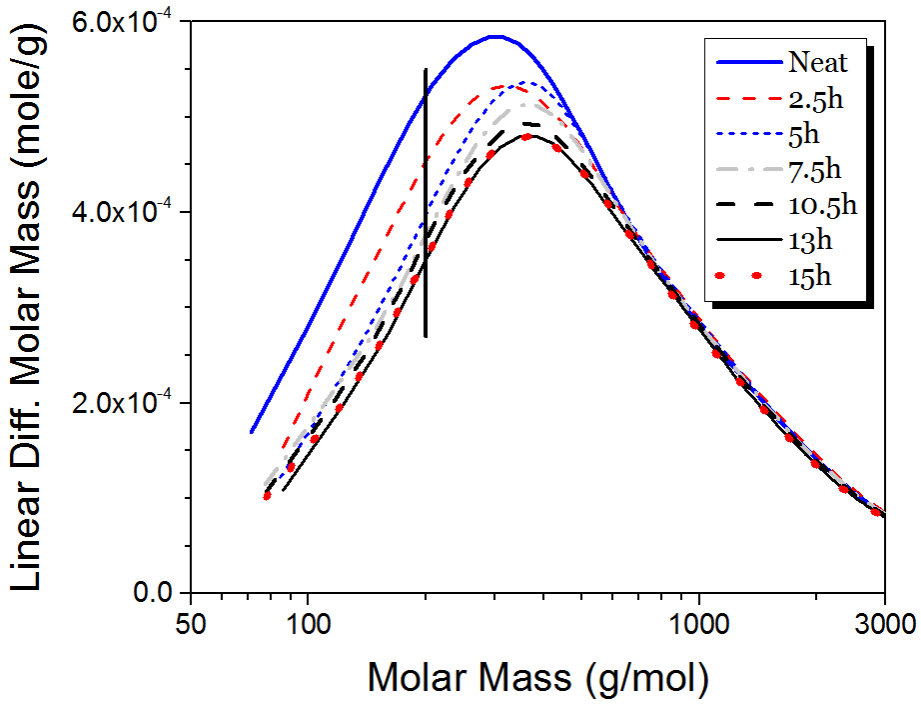

Figure 4. Gel permeation chromatography of as received SMP-10 and after thermal treatment at 86°C in vacuum for increasing time durations. The average MW was observed to shift toward larger MW values and the MW distribution narrowed as the time at temperature increased.

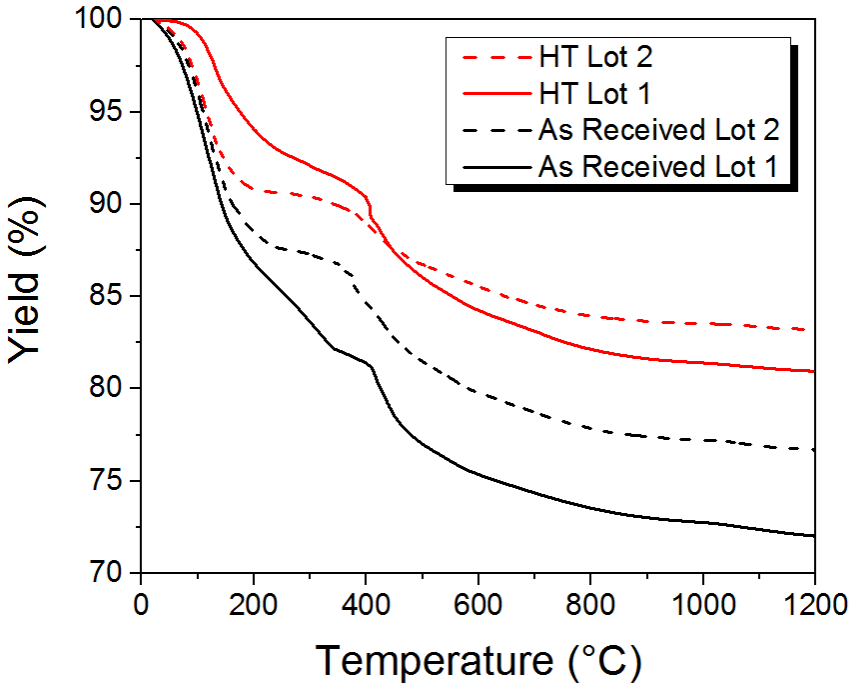

Figure 5. TGA comparison of two lots of SMP-10 (1-solid, 2-dashed) before and after vacuum heat treatment at 90°C for 10 h. The two lots exhibited different thermal behavior and ceramic yields.

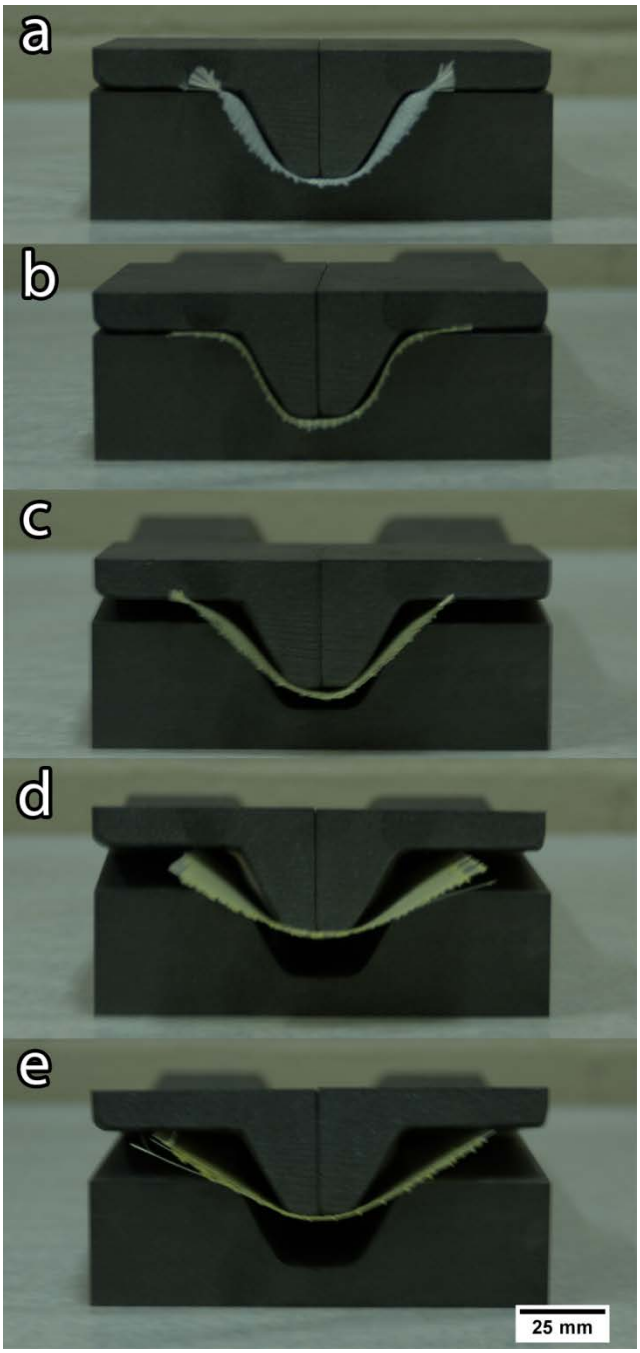

Figure 6. (a) A dry Nextel™ 610 weave conforms to a graphite mold. (b) When loaded with SMP-10 and B-staged for 2 h, the weave retains the ability to conform to the mold contours. The weave increasingly loses the ability to conform to the graphite mold when B-staged for (c) 5 h, (d) 10 h, and (e) 20 h.

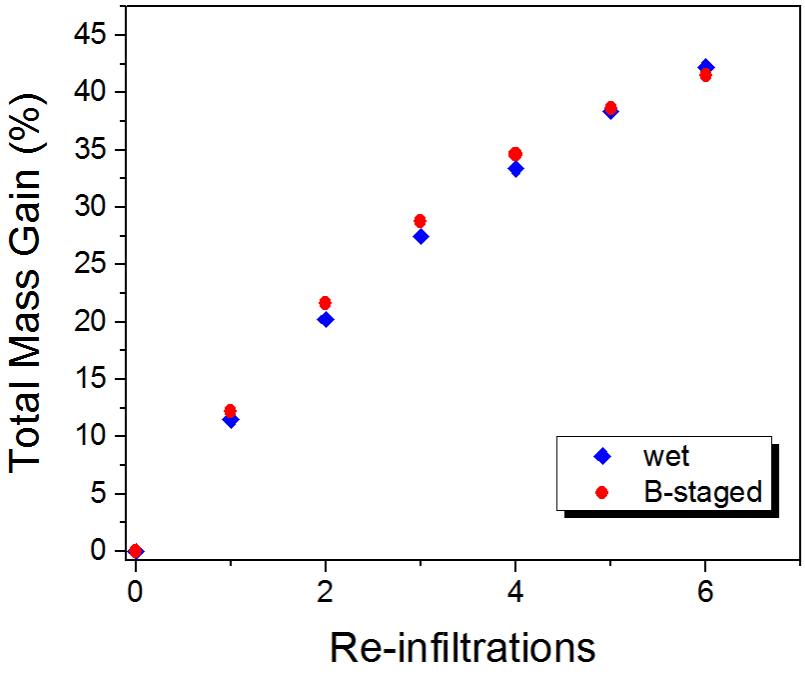

Figure 7. Percent mass gain of wet and B-staged CMC laminates after each re-infiltration.

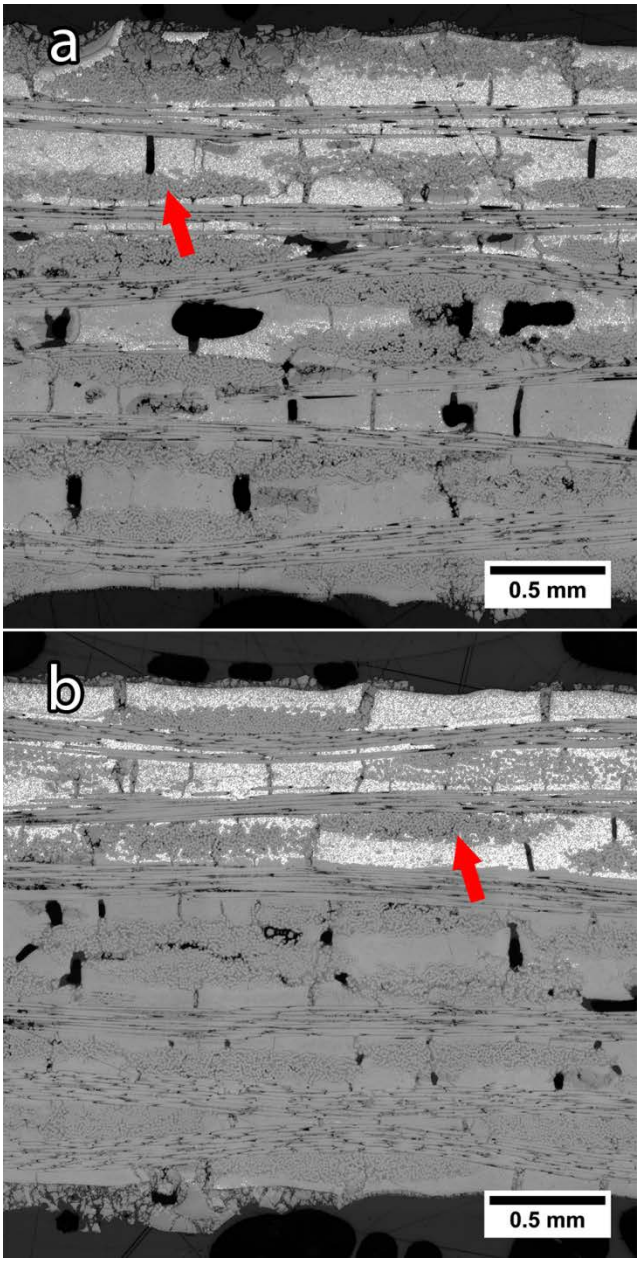

Figure 8. Optical micrograph cross-sections of (a) wet and (b) B-staged CMC laminates with HfB_2 (white) and SiC (grey) particulate loaded layers. HfB_2 was observed to mix at the boundaries of the wet laminate plies. Arrows point to tightly packed tows where HfB_2 particulate infiltration was prohibited.

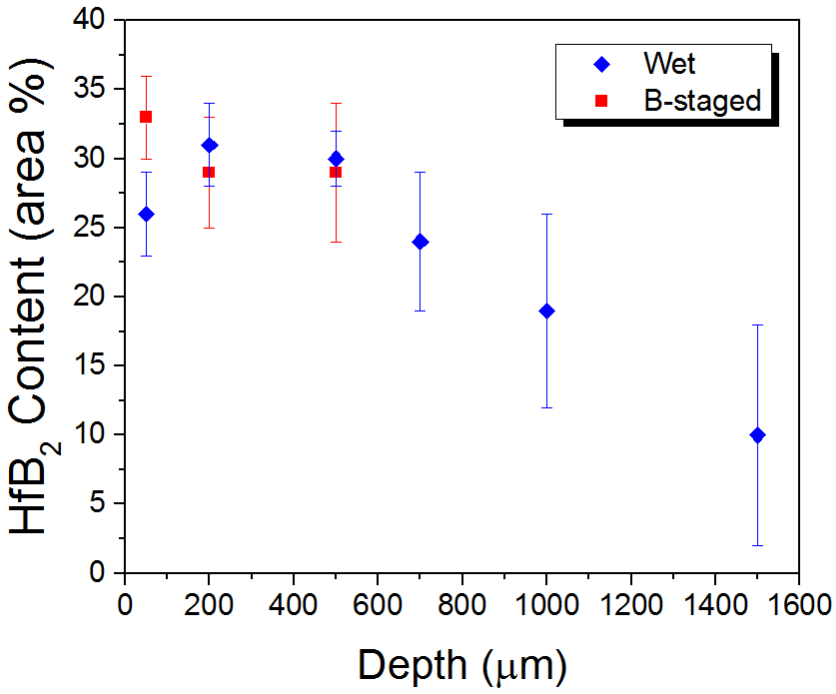

Figure 9. HfB_2 content as a function of depth from the surface for both wet and B-staged CMC laminates.

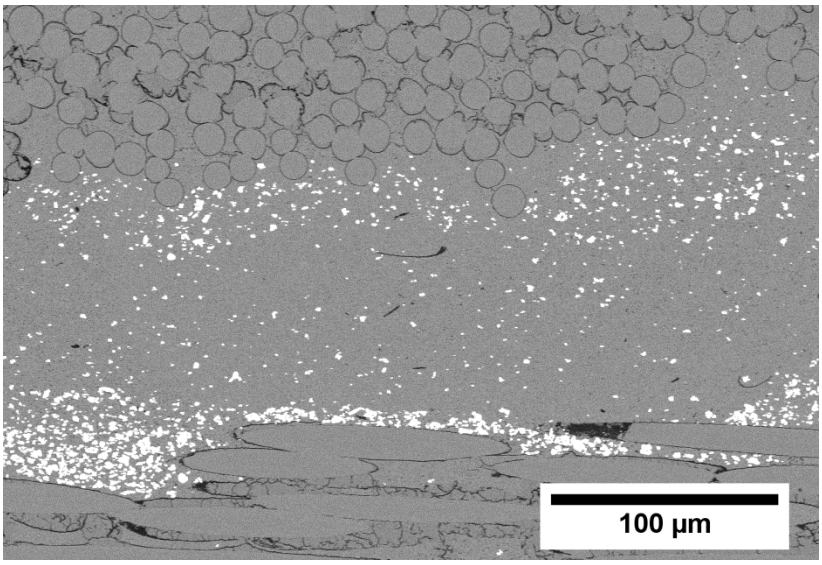

Figure 10. Settling of HfB_2 particulate (white) was observed in the wet CMC laminate, where a higher fraction of HfB_2 rests on the transverse fiber tow than the matrix between the transverse and orthogonal tow.